RSC Advances

ROYAL SOCIETY OF CHEMISTRY

www.rsc.org/advances

Journal Name

ARTICLE

HSA targets multiple Aβ42 species and inhibits the seeding-mediated aggregation and cytotoxicity of Aβ42 aggregates

Received 00th January 20xx,
Accepted 00th January 20xx

DOI: 10.1039/x0xx00000x

www.rsc.org/

Conggang Wang[a], Fang Cheng[*b], Li Xu[a] and Lingyun Jia[*a]

Human serum albumin (HSA) is an important binding partner of amyloid-β (Aβ) in vivo and it can modulate Aβ aggregation. However, the underlying molecular mechanism of this HSA-mediated modulation of Aβ aggregation and cytotoxicity is still not fully understood, especially that of Aβ42, which is the most amyloidogenic and toxic Aβ variant. For this reason, we systematically investigated the effect of HSA on the fibrillation and cytotoxicity of different Aβ42 aggregation species in the amyloid-formation pathways by extensive biophysical and biological tests. Moreover, Surface Plasmon Resonance (SPR) assay was performed to determine the ability of HSA to bind to different Aβ42 species. Collective results indicated several important findings as follows: (i) HSA inhibited the fibrillation of Aβ42 monomer in a concentration-dependent manner; (ii) HSA abolished the seeding ability of protofibril and fibril at 1:1 molar ratio; (iii) HSA interacted with Aβ42 protofibrils and fibrils with increased affinity and formed HSA-Aβ complexes that dissociated at a slower rate than complex formed between HSA and Aβ42 monomer; (iv) HSA prevented seeding-mediated cytotoxicity of Aβ42. Taken together, these findings suggested that the HSA inhibited Aβ42 fibrillation and cytotoxicity through interfering with different stages of Aβ42 fibrillation and targeting different Aβ42 intermediate aggregates. Furthermore, HSA preferentially interacted with Aβ fibrillar aggregates to form slowly-dissociated complexes. These findings contributed to better understanding of the molecular mechanism by which HSA modulates the aggregation and cytotoxicity of Aβ, and provide important implications for further designing HSA-based therapeutic strategies.

Introduction

Alzheimer's disease (AD) is one of the most common incurable neurodegenerative disorders[1, 2]. One pathological hallmark of AD is the accumulation of senile plaques in AD patient brains[3, 4]. The primary components of senile plaques are peptide assemblies by amyloid-β (Aβ)[5, 6]. Aβ is produced through sequential proteolytic cleavage of amyloid precursor protein (APP) by β- and γ-secretases, resulting in two principal Aβ variants: Aβ40 and Aβ42[7, 8]. Aβ40 is the predominant species, but Aβ42 is much more amyloidogenic and toxic, and it is thought to be the culprit involved in the initiation and progression of AD[9, 10]. Accumulating evidence suggests that Aβ aggregation and amyloid formation can trigger a cascade of molecular and cellular events, ultimately leading to the initiation and progression of AD[11, 12].

Aβ aggregation is a typical nucleated-polymerization process that involves primary and secondary nucleation and elongation process, during which many different Aβ aggregates are formed and transformed with different bioactivities [13-16]. In the nucleation phase, Aβ monomers form many oligomers and protofibrils with different structures and morphologies. In the polymerization phase, Aβ protofibrils can further form Aβ fibrils by incorporation of additional monomers/oligomers and also by conformational transformation[17-20].

The nucleation phase can be eliminated by adding preformed fibrillar Aβ aggregates such as Aβ protofibrils and fibrils. The added Aβ aggregates act as seed to accelerate the fibrillation of Aβ monomer in vitro and in vivo[19-21]. The seeding of Aβ aggregates is thought to promote the formation of senile plaques and the propagation of amyloid[21-23]. Recent studies have also demonstrated that seeding mediates the aggregation of amyloid peptides, and this is essential for the cytotoxicity of these peptides, such as Aβ and α-synuclein[14, 20, 24, 25]. Taken together, these studies suggest that seeding-mediated Aβ aggregation plays a key role in AD initiation and progression.

Human serum albumin (HSA) is the most abundant protein in blood plasma, with a concentration of about 640 μM. It acts as a carrier for various small molecules in the blood[26, 27]. HSA has

[a] School of Life Science and Biotechnology, Dalian University of Technology, Dalian 116023, P. R. China. E-mail: lyj81@dlut.edu.cn
[b] School of Pharmaceutical Science and Technology, Dalian University of Technology, Dalian 116023, P. R. China
† Footnotes relating to the title and/or authors should appear here.
Electronic Supplementary Information (ESI) available: [details of any supplementary information available should be included here]. See DOI: 10.1039/x0xx00000x

also been suggested to be the main binding partner of Aβ, and has also been found to be associated with senile plaques deposited in the brain of AD patients. Various reports have suggested that HSA performs a pivotal role in the formation and clearance of Aβ amyloid[26, 28-30]. Despite the significant role in Aβ functions, the underlying mechanism of HSA-mediated modulation of Aβ aggregation and cytotoxicity remains elusive, especially that of Aβ42. Moreover, current understanding concerning the recognition of Aβ species by HSA is still limited and the interaction between HSA and different Aβ species along the aggregation pathways is still largely a subject of debate. For instance, HSA has been found to bind both Aβ40 and Aβ42 monomer at a 1:1 stoichiometry with an equilibrium dissociation constants (K_D) of about 5–10 μM by using immunoassays and circular dichroism (CD)[31, 32] . Some studies have also shown that HSA mainly interacts with nonfibrillar or monomeric form of Aβ, but less interact with Aβ fibrils[33, 34]. However, many NMR studies have shown that HSA does not bind to the monomer of different Aβ variants despite reasonable speculation that Aβ can bind to the hydrophobic pockets within HSA, which are often occupied by fatty acids [30, 35, 36]. Moreover, Surface Plasmon Resonance (SPR) study has also indicated that HSA does not bind to biotin-Aβ40 monomer, but selectively binds to polymeric Aβ42 aggregates[28]. Some reports, on the other hand, indicated that HSA can bind to Aβ 12-28, 40 and 42 oligomers, there appears to be a single high-affinity site for HSA in the Aβ oligomers/protofibrils[30, 35, 36]. Therefore, the binding affinity between HSA and different Aβ species and the kinetics of such interaction remains elusive despite the fact that acquiring such information is critical for the understanding of the mechanisms underlying HSA-mediated modulation of Aβ aggregation and cytotoxicity. Furthermore, while the inhibition of the aggregation of Aβ monomer by HSA have been reported in different studies [28, 33, 34, 37], the inhibitory effects of HSA on the growth of Aβ fibrils as reported are confusing and even contradict[28, 33, 37]. Therefore, whether HSA could act on different aggregation stages and the efficacy of such modulation with respect to different Aβ species need in-depth study.

To untangle this deadlock, this study investigated the effect of HSA on the seeding properties of different Aβ42 aggregates, the interaction between HSA and Aβ42, and the effect of HSA on Aβ42-induced cytotoxicity. Collective results showed that HSA targeted multiple Aβ42 species, interacted with these peptides with distinct affinity and kinetics, and potently inhibited seeding-mediated Aβ42 aggregation and cytotoxicity. These findings contribute to better understanding of the molecular mechanisms by which HSA modulates the aggregation and cytotoxicity of Aβ42, and may provide new insights into the further development of HSA-based therapeutic strategies.

Experimental

Chemicals

Human Aβ1-42 with more than 95% purity was purchased from Chinese Peptide Company (Hangzhou, China). HSA (99% purity, fatty acid free and essentially globulin free), dimethyl sulfoxide (DMSO), N-hydroxysuccinimide (NHS), N-(2-dimethylaminopropyl)-N'-ethyl-carbodiimide (EDC), ethanolamine and thioflavin T (ThT) were purchased from Sigma-Aldrich (MO, USA). Sodium 8-Anilino-1-naphthalenesulfonate (ANS-Na) was purchased from Tokyo Chemical Industry Co., Ltd. (Tokyo, Japan). All other chemicals used were of analytical grade unless otherwise stated. MilliQ water was used to prepare buffers and all of the buffers were filtered through a 0.22-μm syringe filter before use. Filtration chromatography column G50 HP was purchased from Beijing Weishibohui Chromatography Technology Co., Ltd (Beijing, China).

Preparation of Aβ42 crude (CR) solution

Aβ42 crude solution (CR) which consists of a mixture of Aβ42 protofibrils and monomers, was prepared as described previously[14, 20]. Briefly, 50 μL of 100% anhydrous DMSO was used to completely solubilize 1 mg of lyophilized Aβ42 peptide powder. Then, 800 μL of MilliQ water was immediately added to the solution followed by the addition of 10 μL of 2 M Tris-HCl (pH 7.6). The Aβ42 CR solution was kept at room temperature for 15 min and then used immediately.

Preparation of Aβ42 protofibril and monomer

To prepare the Aβ42 monomer, 1 mg of lyophilized Aβ42 peptide powder was solubilized in 1 ml of 6 M guanidine HCl solution and then centrifuged at 14,000×*g*/4℃ for 15 min. After that, 75% of the supernatant was collected and subjected to size-exclusion chromatography (SEC). SEC was conducted using a G50 HP column (separation range: 1000-30000) coupled to an ÄKTA purifier 100 system (GE Healthcare, USA). The column was equilibrated with 10 mM Tris-HCl (pH 7.4) or 10 mM PBS (pH 7.4) prior to the injection of the Aβ sample. After injection of the sample, the column was eluted at a flow rate of 0.5 ml/min and the absorbance of the eluent was monitored by absorbance at 214 nm and 280 nm. Aβ42 aggregates were eluted within the void volume whereas Aβ42 monomers were eluted within the 17-19 ml peak as described previously[15, 19, 20]. To obtain both Aβ42 protofibril and monomer, the Aβ42 CR solution was prepared as described above. After centrifugation at 14,000×*g*/4℃ for 15 min, 75% of the supernatant was collected and fractionated on a G50 HP column as described above. The fractions eluting in the void volume were combined and labelled as Aβ42 protofibril and the fractions eluting at 17-19 ml peak were combined and labelled as Aβ42 monomer. The Aβ42 monomers and Aβ42 protofibrils were used immediately for aggregation and SPR studies.

Preparation of Aβ42 fibrils

To prepare Aβ42 fibrils (F), Aβ42 CR solution (200 μM) was incubated for 48 h in a 37 °C orbital shaker incubator set at 100 rpm as described previously[20]. To prepare Aβ42 fibril seed solution for SPR studies, the prepared Aβ42 fibril was collected by centrifugation for 30 min at 14,000×*g*/4℃ and washed twice with water. The collected Aβ42 fibril was resuspended in

water and then kept on ice while being sonicated with a microprobe using 15 intermittent pulses (0.6-s pulses, 0.4-s interval, output level 2) as described previously[38, 39]. The quality of the Aβ42 fibril sample was confirmed by ThT assay and TEM observation.

Aβ concentration determinations

The concentration of the Aβ preparation was determined by Bradford assay as previously described[40].

ThT assay

ThT powder was first dissolved in water to a final concentration of 4 mM. This stock solution was then filtered and diluted in PBS buffer to a working concentration of 25 μM. The ThT assay was performed by mixing 20 μL of Aβ with 180 μL ThT working solution in a black 96-well plate. The ThT fluorescence was measured in triplicate using a Varioscan Flash Spectrofluorometer (Thermo Scientific) with excitation and emission at 450 and 482 nm, respectively. The average fluorescence intensity was calculated as described previously[37, 41], after subtracting the signal of control sample (without Aβ peptide). All ThT fluorescence experiments were conducted at 25℃.

ANS assay

ANS powder was solubilized in MilliQ water to a final concentration of 4 mM. The ANS stock solution was further diluted in 30 mM citrate buffer (pH 2.6) to a working concentration of 25 μM, and 180 μL of this ANS working solution was mixed with 20 μL Aβ in a black 96-well plate. The sample was excited at 350 nm and the emission spectrum was measured at 400 to 600 nm using a Varioscan Flash (Thermo Scientific Co.). All ANS fluorescence experiments were conducted at 25℃.

Transmission electron microscopy

An aliquot (10 μL) of the Aβ sample was allowed to adsorb onto a carbon-coated copper grid (400 mesh) for 10 min. After washing with 10 μL MilliQ water twice, the grid was negatively stained with 2% phosphotungstic acid for 1 min and again washed with 10 μL MilliQ water and then dried by air. At each step, the excess liquid was first blotted off with filter paper. The sample was then analyzed using a Tecnai G220 S-Twin or a JEM-2100 at 200 kV.

Aβ fibrillation studies

To investigate the effect of HSA on the aggregation of Aβ42 monomers (M), 15 μM of Aβ42 M was incubated in the absence or presence of different concentrations of HSA at 37 ℃ with shaking at 100 rpm. For seeding study, Aβ42 M solution was mixed with Aβ42 protofibril (PF) or fibril (F). Three groups of samples were prepared. The positive control group consisted of 4 μM Aβ42 PF + 20 μM Aβ42 M, 4 μM Aβ42 F + 20 μM Aβ42 M, and 20 μM Aβ42 crude (CR) solution only. The test group consisted of essentially the same three sets of samples as in the positive control group, but in addition, each sample also contained 4 μM HSA. The negative control group consisted of 20 μM Aβ42 M or 4 μM HSA only. All samples were incubated at 37℃ without agitation and the formation of Aβ42 F was examined by ThT fluorescence assay and TEM analysis as described above.

Surface Plasmon Resonance measurement

All runs were conducted on a Biacore X100 processing unit using 10 mM Hepes (pH 7.4) containing 150 mM NaCl, 3 mM EDTA and 0.005% (v/v) Tween 20, both as a running buffer and a diluent. Aβ42 monomers, protofibrils and sonicated fibrils were each diluted with 10 mM sodium acetate (pH 4.0) and immobilized on a Biacore CM5 sensor chip via an amine coupling method, performed according to the manufacturer's protocol. Non-reacted but activated sites on the sensor chip were blocked with 1 M ethanolamine. The reference channel was prepared by immobilizing bovine serum albumin (BSA) on the sensor chip as described previously[42]. The coupling levels were 549.4-2169.1 response units (RU) for Aβ42 species and 6785.6-7901.7 RU for BSA. HSA was diluted to 0.5 – 50 μM and passed over the flow cells at a flow rate of 30 μL/min to minimize the mass transfer effect for kinetics study. The association time was 60 s and the dissociation time was 180 s. The Aβ42 monomers and protofibrils immobilized sensor chips were regenerated by washing the system with 0.2 M glycine (pH 2.0) for 30 s between runs and the Aβ42 fibrils-immobilized sensor chip was regenerated with 0.2 M glycine (pH 1.5) for 30 s between runs. The binding data omitted any noise at the beginning and end of analyte injection and then double referenced. The data were fitted to a 1:1 binding model using the global fit option in Bioevalution analysis software.

Cell viability assays

Human neuroblastoma cell line SH-SY5Y (ATCC) was cultured in DMEM (Gibco) supplemented with 10% fetal bovine serum and 1% penicillin/streptomycin (Gibco). The cells were plated in 96-well cell culture plate at a density of 8×10^3 cells per well and allowed to grow in a cell culture incubator (37 °C; ambient humidity; 5% CO_2) for 24 h. After that, the culture medium was removed, and the cells were washed with PBS twice and fresh DMEM/N2 supplemented with 1% penicillin/streptomycin (Gibco) was added to the cells and cultured for another 12 h. Next, Aβ42 CR was added to the cells to a final concentration of 10 or 20 μM, with or without the addition of HSA (final concentration 2.5-80 μM) followed by 48 h of incubation. Finally, the viability of the cells was assessed by standard 3-(4,5-dimethylthiazol-2-yl)-2,5-dephenyltetrazolium bromide (MTT) reduction assay and an Alamar Blue assay.

In the case of MTT reduction assay, the culture medium was removed and the cells were washed twice with PBS buffer, followed by the addition of fresh DMEM and 10 μL of MTT solution (5mg/ml) and 3-h incubation. After that, the culture medium was removed and replaced with 150 μL of DMSO and further incubated for 30 min, and the absorbance of the plate was then measured at 570 nm (630 nm was used as a reference wavelength) using a microplate reader (TECAN). Cell viability was expressed as percentage relative to that of control (cells not treated with Aβ42).

In the case of Alamar Blue assay, after the cells were treated with the Aβ-HSA mixture for 48 h, they were then washed twice with pre-warmed fresh medium and incubated with 10%

(v/v) Alamar Blue (KeyGEN BioTECH, China) in fresh medium for 3 h. Cell viability was determined by measuring the extent of cellular metabolic reduction of Alamar Blue, which was achieved by recording the fluorescence of the sample at an excitation wavelength of 530 nm and an emission wavelength of 590 nm using a Varioskan Flash (Thermo Scientific Co.). Cell viability was expressed as the percentage of the signal obtained for the control.

Statistical analysis

All data were presented as the means ± standard deviations (SDs). Statistical analysis was conducted using one-way ANOVA test.

Results and discussion

Preparation and characterization of different Aβ42 species

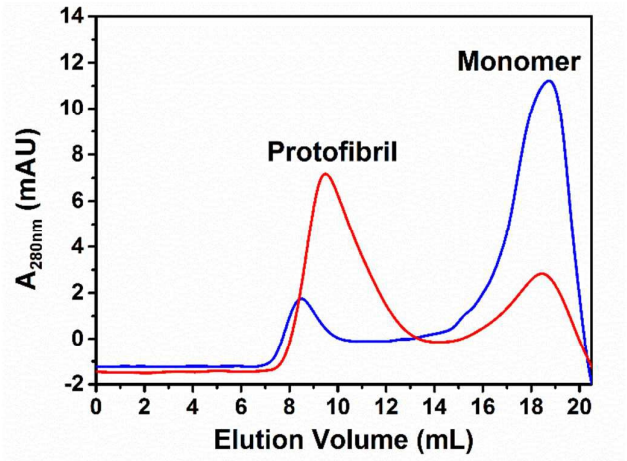

Fig. 1 Preparation of Aβ42 protofibril and monomer. Fractionation of Aβ42 into protofibril (red line-using DMSO solubilization method) or monomer (blue line-using 6 M guanidine HCl solubilization method) on a G50 HP size-exclusion chromatography column.

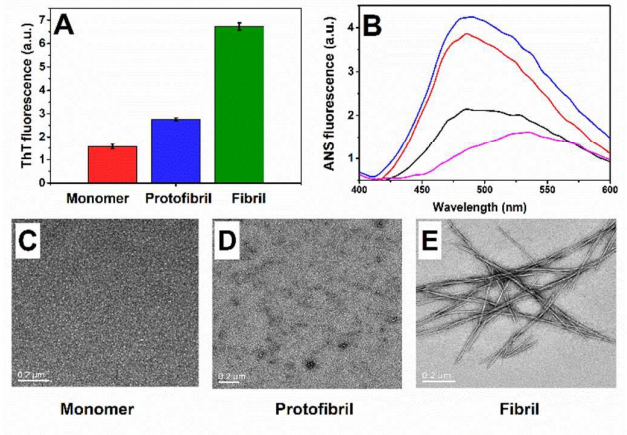

Fig. 2 Characterization of different species of Aβ42. (A) ThT fluorescence intensity of 15 μM of Aβ42 monomer, protofibril and fibril. ThT signals were acquired after incubating the Aβ42 samples with ThT working solution for 1 min. Data are the means [in arbitrary units (a.u.)] ± SDs from triplicate samples. (B) ANS fluorescence spectra obtained with buffer (pink) and 15 μM of Aβ42 monomer (black), protofibril (red) and fibril (blue). TEM images of Aβ42 monomer (C), protofibril (D), and fibril (E). The scale bars in TEM images represent 200 nm.

To investigate the effect of HSA on the aggregation and cytotoxicity of different Aβ42 species, Aβ42 monomers (M), protofibrils (PF) and fibrils (F) were first prepared and characterized. Aβ42 was chosen in the present study not only because it is the most amyloidogenic and toxic Aβ variant, but also Aβ42 protofibrils and fibrils could be produced in high quantities using recently reported procedures[15, 19, 20]. Depending on the purification method, separation by SEC using a G50 HP column would yield either dominantly Aβ42 monomers or a monomer fraction and a second fraction consisting of a heterogeneous mixture of Aβ aggregates of different sizes, namely Aβ42 protofibrils **(Fig. 1)**. In the separation process, either Tris or PBS running buffer was used, depending on the purpose of later experiments. Tris buffer was not appropriate for amine coupling reactivity in SPR measurement, therefore PBS was used as elution buffer in the separation of Aβ42 PF and M. Aβ42 F was produced by gently agitating Aβ42 crude (CR) solution at 37 °C because in this condition, aggregate formation and conversion to Aβ42 F could readily happen. ThT is a well-known indicator for recognizing the cross β-sheet structure of Aβ42 F. The intensity of ThT binding was proportional to the quantity of cross β-sheet structure in Aβ F. Aβ protofibrils exhibit pronounced ThT fluorescence, despite less than an equimolar solution of Aβ fibrils, while Aβ monomers and low molecular weight oligomers do not generate ThT fluorescence.[15, 18, 20]. The sample of Aβ42 CR agitated for 48 h showed significant ThT binding, which indicated the formation of Aβ42 F with substantial cross β-sheet structure. The ThT signal of Aβ42 M was lowest, and this demonstrated that the Aβ42 M preparation was devoid of Aβ aggregate, which contained β-sheet structure. Binding of ThT by Aβ42 PF was less pronounced compared to Aβ42 F despite the fluorescence signal of Aβ42 PF plus ThT sample being higher than that of Aβ42 M plus ThT sample **(Fig. 2A)**. This confirmed the presence of less-orderly stacked β-sheet structure in Aβ42 PF, consistent with previous studies[19, 20, 43]. ANS is highly sensitive to the exposed hydrophobic regions in native or partially unfolded proteins, and therefore it is able to probe the hydrophobicity of distinct Aβ species. The binding of ANS to solvent-exposed hydrophobic patches results in enhancement of ANS fluorescence intensity and a blue shift of the maximum fluorescence emission [43]. The addition of all Aβ42 species to ANS solution led to pronounced blue shift in maximum fluorescence emission (from 530 nm to 485 nm) and significant increase in fluorescence intensity compared to the blank sample (no Aβ42) **(Fig. 2B)**. In the presence of ANS, the fluorescence intensity produced by Aβ42 F was the highest followed by the intensity of Aβ42 PF, while Aβ42 M produced the least fluorescence intensity **(Fig. 2B)**. The results indicated that Aβ42 PF and F contained more exposed hydrophobic patches. The different Aβ42 species had quite distinct

morphologies as revealed by TEM. The Aβ42 M preparation showed the absence of any recognizable aggregates **(Fig. 2C)**, whereas Aβ42 PF consisted of a heterogeneous mixture of globular aggregates of different diameters (10-20 nm) and curvilinear Aβ aggregates with an average diameters of 8-10 nm and a length of 25-40 nm **(Fig. 2D)**, while Aβ42 F preparation contained a network of mature fibrils **(Fig. 2E)**. The different Aβ42 species prepared were therefore structurally and morphologically distinct from each other.

HSA suppresses the fibrillation of Aβ42 monomer in a concentration-dependent manner

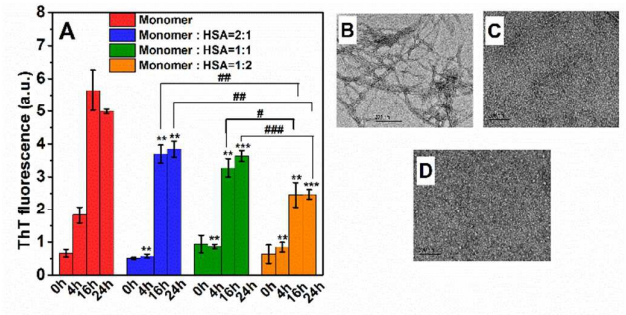

Fig. 3 Time-dependent inhibition of Aβ42 monomer fibrillation by HSA. (A) ThT fluorescence intensity observed for the aggregation of 15 μM Aβ42 monomer in the absence or presence of 7.5 μM, 15 μM or 30 μM of HSA at 37℃ with shaking at 100 rpm. Data are the means [in arbitrary units (a.u.)] ± SDs from triplicate samples. TEM images of 15 μM Aβ42 monomer (B), 15 μM Aβ42 monomer plus 30 μM of HSA (C) or 30 μM of HSA (D) taken at 24 h. The scale bars in TEM images represent 200 nm. (one way ANOVA; *, $p<0.05$; **, $p<0.01$; ***, $p<0.001$ as compared to ThT intensity of Aβ42 monomer alone. #, $p<0.05$; ##, $p<0.01$; ###, $p<0.001$ for the pairs of data sets).

The effect of HSA on the fibrillation of Aβ42 monomers was studied by monitoring the changes in ThT fluorescence of a mixture containing HSA and Aβ42 monomer. The aggregation of Aβ42 monomers was induced by gentle agitation of a mixture of Aβ42 monomers and HSA at 1:2, 1:1 or 2:1 molar ratio of Aβ42 monomer to HSA. Previous studies have confirmed that the presence of serum albumin does not interfere with the detection of Aβ fibrils by ThT assay [37]. Aβ42 incubated in the absence of HSA showed a significant increase in ThT fluorescence over time, suggesting the formation of Aβ42 fibrils with cross β-sheet structure. Maximum fluorescence occurred at 16 h, followed by slight decrease at 24 h. The reason for this slight ThT decrease could be attributed to twist and entanglement of the Aβ fibrils. This observation was not surprising since some studies have already indicated decreased ThT signal after reaching a maximum value, a feature that has been suggested to be attributed to the interaction between Aβ fibrils and the precipitated aggregates [37, 44, 45]. Incubating Aβ42 monomers in the presence of different concentrations of HSA led to decreased ThT intensity at each time point. The decrease in ThT intensity was a consequence of reduced production of Aβ fibril. Furthermore, the inhibitory effect of HSA on the aggregation of Aβ42 monomers improved significantly with increasing concentrations of HSA. Incubation of 15 μM Aβ42 monomer in the presence of 7.5, 15 and 30 μM of HSA inhibited the monomer fibrillation by 23%, 27% and 51%, respectively **(Fig. 3A)**. Therefore, the inhibitory effect of HSA on Aβ42 monomer aggregation was more significant at higher concentrations of HSA. Several literatures have also reported more pronounced inhibitory effect of serum albumin on Aβ monomer aggregation at high concentrations of serum albumin [34, 37]. The relatively weak inhibitory effect on Aβ42 monomer aggregation at low concentrations of HSA might be due to two possible reasons: (1) weak interaction between HSA and Aβ42 monomer, which have been suggested in many studies [28, 31, 32] or (2) the efficient prevention of the emergence of amyloid seeds may require a minimal inhibitor concentration, since the Aβ aggregation is initiated by the incidental appearance of amyloid seed in the solution. In our case, HSA at low molar ratios (1:2 and 1:1) may be insufficient to entirely prevent the appearance of the Aβ seeds in the solution, thus conferring a low inhibitory effect on Aβ aggregation. In agreement with the ThT data, TEM assay also showed that Aβ42 monomers formed dense fibril network after 24 h of agitation **(Fig. 3B)**. In contrast, the aggregation of 15 μM Aβ42 monomer in the presence of 30 μM HSA produced very few Aβ fibrils, and only dispersed and isolated Aβ fibrils were observed (**Fig. 3C)**. In addition, when HSA was incubated in the absence of Aβ42, no aggregate or fibril formation was observed **(Fig. 3D)**. Therefore, it could be concluded that HSA inhibited Aβ42 monomer aggregation in a concentration dependent manner. Aβ fibrillation is a nucleated polymerization process which involves the formation of protofibril intermediates. The protofibrils further aggregate and convert to Aβ fibrils. Aβ protofibrils and fibrils became longer upon the addition of Aβ monomers, resulting in rapid increase in ThT fluorescence[19, 20, 46]. Therefore, the inhibitory effect of HSA on Aβ42 fibrillation could be attributed to the capacity of HSA to target Aβ42 monomers or Aβ42 aggregates such as protofibril or fibrils or both. The mechanism involved in the modulation of Aβ42 aggregation by HSA was further elucidated by investigating the effect of HSA on the seeding properties of different Aβ42 aggregates.

HSA abolishes the seeding property of Aβ42 protofibrils and fibrils

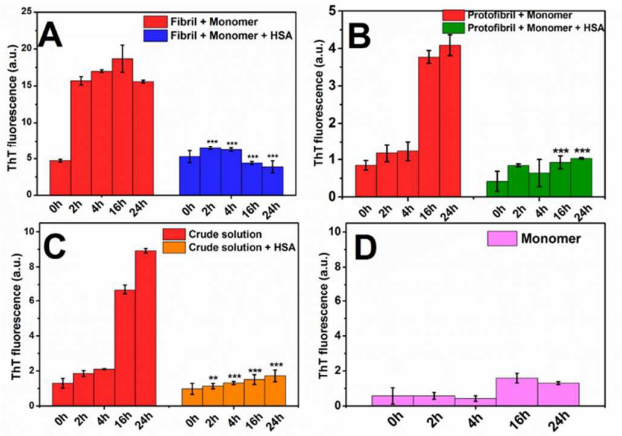

Fig. 4 HSA abolishes the seeding properties of Aβ42 protofibril and fibril. ThT fluorescence intensity at different time points of the aggregation process at 37℃ without agitation. (A) 20 μM Aβ42 monomer seeded with 4 μM Aβ42 fibrils in the absence/presence of 4 μM HSA. (B) 20 μM Aβ42 monomer seeded with 4 μM Aβ42 protofibril in the absence/presence of 4 μM HSA. (C) 20 μM Aβ42 crude solution in the absence/presence of 4 μM HSA. (D) 20 μM Aβ42 monomer alone. Data are the average fluorescence intensity [in arbitrary units (a.u.)] ± SD from triplicate samples. (one way ANOVA; *, $p<0.05$; **, $p<0.01$; ***, $p<0.001$ as compared to ThT intensity of Aβ42 monomer seeded with Aβ42 aggregates or Aβ42 crude solution in the absence of HSA.)

To further investigate the effect of HSA on the aggregation of different Aβ42 species, the ability of HSA to modulate the seeding capacity of Aβ42 aggregates was studied. The formation of fibrils can be accelerated by the addition of aggregating seeds such as Aβ protofibrils or fibrils at the beginning of the aggregation process. Aβ protofibril represents a mixture of Aβ aggregates with different sizes and morphologies, and contains globular and chain-like species[20, 43, 47]. As depicted in **Fig. 4 (D)**, the ThT fluorescence of sample containing Aβ42 monomers alone did not increase significantly over the entire 24-h incubation at 37℃ under quiescent condition. The result indicated that formation of Aβ42 fibrils by incubating Aβ42 monomers alone was not significant under the present experimental timescale. This is not surprising as previous study has shown that no significant aggregation occurs in a short time under low concentration of Aβ monomer unless the sample is agitated[48]. Thus the Aβ42 monomers purified by SEC were homogenous and free of Aβ aggregates. In the sample in which 20 μM Aβ42 monomer was co-incubated with preformed Aβ42 protofibrils or fibrils, immediate increase in ThT fluorescence was observed upon the addition of 4 μM Aβ42 protofibril or fibril **(Figs. 4A & 4B)**, indicating the addition of Aβ protofibrils or fibrils to the Aβ monomers significantly accelerated the fibrillation of Aβ monomers. Interestingly, addition of HSA to the mixture of Aβ42 monomers and Aβ42 protofibrils or Aβ42 fibrils significantly inhibited the increase in ThT fluorescence over time, indicating that the seeding capacity of Aβ42 protofibrils and fibrils had been abolished. To further confirm the finding, the effect of HSA on the aggregation of Aβ42 crude (CR) solution was assessed. Incubation of Aβ42 CR without HSA resulted in significant increase in fluorescence over time, indicating that the Aβ42 protofibrils present in the Aβ42 CR solution acted as seed to promote the aggregation of Aβ42 monomers **(Fig. 4C)**. Recent studies have also shown that Aβ42 CR can undergo much more extensive fibrillation than purified Aβ42 protofibrils and monomers[20, 49, 50]. The addition of HSA to Aβ42 CR also reduced the increase in ThT fluorescence, which suggested that HSA could also inhibit Aβ42 CR fibrillation, further demonstrating that HSA could efficiently abolish the seeding capacity of Aβ42 aggregates **(Fig. 4C)**. Moreover, the ThT fluorescence was not reduced when HSA was added to samples consisted of Aβ42 monomers plus Aβ42 protofibrils/fibrils or to Aβ42 CR sample, suggesting that HSA did not cause the disaggregation of Aβ protofibrils and fibrils under the present experimental conditions (**Fig. 4 A-4C)**.

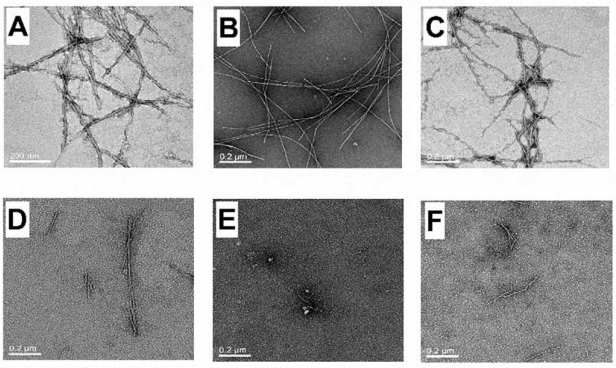

Fig. 5 TEM images showing the reduced formation of Aβ fibrils upon addition of HSA to the Aβ mixture. (A) 20 μM Aβ42 monomer seeded with 4 μM Aβ42 fibrils. (B) 20 μM Aβ42 monomer seeded with 4 μM Aβ42 protofibril. (C) 20 μM Aβ42 crude solution. (D) 20 μM Aβ42 monomer seeded with 4 μM Aβ42 fibril in the presence of 4 μM HSA. (E) 20 μM Aβ42 monomer seeded with 4 μM Aβ42 protofibril in the presence of 4 μM HSA. (F) 20 μM Aβ42 crude solution in the presence of 4 μM HSA. Images are representatives of 20 examined fields. Scale bar in the images represents 200 nm.

Consistent with the results of ThT assay, TEM analysis also revealed, in the absence of HSA, the presence of dense fibril network in the samples containing Aβ42 monomers plus Aβ42 protofibrils or Aβ42 fibrils **(Fig. 5A & 5B)**, but only isolated short fibrils were found in samples containing Aβ42 monomers plus fibrils in the presence of HSA **(Fig. 5D)**. Moreover, when the mixture containing Aβ42 protofibrils and monomers or Aβ42 CR was incubated with HSA, the aggregates mainly consisted of short flexible protofibrillar structures similar to Aβ protofibrils **(Fig. 5E & 5F)**. Furthermore, the formation of Aβ amorphous aggregates was not observed in all samples upon the addition of HSA. Therefore, it could be deduced that HSA did not direct Aβ toward the formation of amorphous aggregates, a function that is afforded by some small drug molecules[51, 52]. Taken together, our results suggested that HSA could target multiple Aβ42 species on the amyloid pathway to inhibit their aggregation. Furthermore, HSA may preferentially interact with Aβ aggregates because it potently inhibited the seeding of Aβ aggregates at a 1:1 HSA to Aβ42 protofibrils/fibrils molar ratio.

Currently, it remains unclear whether HSA interacts more avidly with Aβ monomer or protofibrils or fibrils as there have been inconsistent results appearing in the literatures. There is also far less information about the binding kinetics between HSA and different Aβ species despite the fact that this kind of study can provide essential information to better understand the underlying mechanism involved in the interaction between HSA and Aβ. HSA displayed ＞ 74% inhibition of the seeding-mediated aggregation of the Aβ42 aggregate in equal molar ratio **(Fig. 4A-4C)**, compared to just 27% inhibition when HSA was added to the Aβ42 monomer, also at a 1:1 molar ratio **(Fig. 3A)**. This suggested that HSA might preferentially bind to the intermediates of the aggregation process.

Binding of HSA to different Aβ42 species

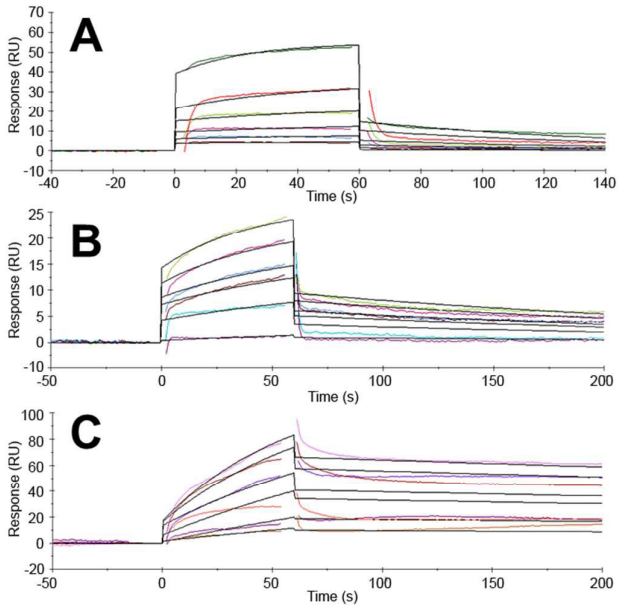

Fig. 6 Sensorgram showing the binding of HSA to different immobilized Aβ42 species. (A) Binding of HSA to immobilized Aβ42 monomer. Concentrations of HSA used: 1, 2.5, 5, 10, 25 and 50 μM. (B) Binding of HSA to immobilized Aβ42 protofibril. Concentrations of HSA used: 1.25, 5, 8, 10, 15 and 20 μM. (C) Binding of HSA to immobilized Aβ42 fibril. Concentrations of HSA used: 0.5, 1, 2, 2.5, 4 and 5 μM. The data were double referenced and globally fit to a 1:1 Langmuir binding model. Sensorgrams are shown as colored lines and the fits were shown as black lines.

Table 1: Kinetic constants of HSA from its reaction with Aβ42 monomers (M), protofibrils (PF) and fibrils (F) obtained via SPR

ligand immobilized	K_a ($\times 10^2$) (M^{-1} s^{-1})	K_d ($\times 10^{-2}$) (s^{-1})	K_D (μM)
Aβ42 M	7.12±1.32	1.20±0.25	17.53±6.08 (7.04%)
Aβ42 PF	13.17±2.48	0.42±0.03	3.28±0.45 (6.30%)
Aβ42 F	33.04±1.67	0.09±0.05	0.29±0.17 (4.50%)

Chi^2 (χ^2) values are indicated in brackets.

SPR is a powerful tool to elucidate the binding kinetics of macromolecules. The binding process of two macromolecules can be studied in real time and without the need to label the molecules[53, 54]. To minimize the risk of further interaction between different Aβ42 species and possible structural rearrangements in the solution, Aβ42 monomers, protofibrils and fibrils were immobilized onto a sensor chip as ligands. The SPR data obtained indicated that binding between HSA and immobilized Aβ42 monomer, protofibril or fibril was specific, and each with different kinetic pattern and affinity. **Figure 6 (A, B and C)** shows the curves for the experimental and theoretical fits of the binding between HSA and different species of Aβ42. The kinetic parameters obtained from a 1:1 Langmuir fit of association and dissociation phases are given in **Table 1**. According to the equilibrium dissociation constants (K_D) for the binding between HSA and each of the three species of Aβ42, HSA appeared to have a significantly higher affinity for Aβ42 aggregate than for Aβ42 monomer. Furthermore, HSA exhibited a higher affinity for Aβ42 fibril than for Aβ42 protofibril. This may suggest that the affinity between HSA and Aβ probably increased as the aggregation process proceeded. In addition to showing the affinity between two molecules, SPR can also provide important information about the binding kinetics, which is very useful for studying the mechanism of the interaction between two molecules. A high dissociation rate constant indicates the complex formed by two molecules is unstable and tends to dissociate rapidly. The different binding kinetics constants obtained for the binding between HSA and different species of Aβ indicated that the exact binding pattern was characteristic of the Aβ species itself. The dissociation rate constant for the binding between HSA and Aβ42 aggregate was significantly lower than that between HSA and Aβ42 monomer **(Table 1)**. Furthermore, lower dissociation rate constant was obtained for the binding between HSA and Aβ42 fibril than for the binding between HSA and Aβ42 protofibril. Therefore, HSA-Aβ aggregate complex was more stable than HSA-Aβ monomer complex, and HSA-Aβ fibril complex was the most stable among the three HSA-Aβ species complex.

Despite the significance of HSA-Aβ interaction, current understanding concerning the interaction between HSA and different Aβ species is still limited due to the inconsistency in the reported experimental data. In the case of HSA/Aβ42 monomer binding, the K_D obtained from SPR analysis was approximately 17.5 μM, which was similar to the reported K_D of 5-10 μM obtained for the binding between HSA and Aβ40 and between HSA and Aβ42 monomer, both at 1:1 molar ratio, as measured by CD, immunoassay or ThT assay[26, 31-33], but was one order of magnitude higher than the K_D obtained for the binding between HSA and Aβ42 monomer obtained by SPR in a recent study[42]. Nevertheless, recent NMR studies have shown that HSA does not bind to Aβ12-28, 40 and 42 monomers and the authors deduced that presence of Aβ oligomer in the sample is an important factor that can interfere with the measurement[30, 35, 36]. To rule out the possibility of Aβ oligomer present in the samples, Aβ monomers were acquired through a process that consisted of guanidine HCl solubilization and

SEC purification, a process that could ascertain the monodisperisity of the preparation[15, 20] and the acquired Aβ monomers were immobilized immediately onto the sensor chip to reduce the risk of possible further aggregation. Therefore, the possible interference from high-molecular-weight Aβ oligomers could be greatly reduced, and the result obtained better demonstrated that HSA could specifically bind to Aβ42 monomer. The weaker affinity observed in our study compared to the affinity reported in recent SPR study[42] (10^{-5} versus 10^{-6} M of magnitude) could be attributed to the different methods used to prepare the Aβ sample. In that SPR study, 1,1,1,3,3,3-Hexafluoro-2-propanol (HFIP) treated Aβ peptide film was redissolved in DMSO and further diluted into 10 mM sodium acetate at pH 5.5 for immobilization[42]. It should be noted that the isoelectric point of Aβ is 5.5, and hence the immobilization buffer used could induce the formation of some Aβ aggregates with amorphous structure as reported[55, 56]. Moreover, recent studies have shown that HFIP-treated Aβ42 can form Aβ aggregates immediately upon further dilution in buffer[57, 58]. Therefore, it was necessary to isolate Aβ42 monomers from Aβ42 aggregates by SEC prior to further analysis. The stronger affinity reported by previous SPR study (K_D of 10^{-6} M of magnitude) might be attributed to traces of Aβ aggregates with uncertain structure that had also been immobilized.

Despite HSA having higher affinity for Aβ42 amyloid than for monomer, it exhibited a stronger affinity for Aβ42 fibril than for protofibril, probably because of the structural difference in Aβ42 fibril and protofibril. Aβ protofibrils represent aggregating intermediates which have a higher level of β-structure, with more exposed hydrophobic patches than Aβ monomer but have a lower level of β-structure and less exposed hydrophobic patches than Aβ fibrils. The transition from Aβ protofibril to fibril is accompanied by a massive structural reorganization and the non-fibrillar structure present in Aβ protofibril is transformed into fibrillary β-structures during the aggregation process[17, 18, 59-62]. Furthermore, our data indicated that Aβ42 fibrils grew faster than protofibrils when monomers were added, consistent with the finding of recent studies[63, 64]. The data therefore suggested that during the overall structural conversion of Aβ protofibrils to fibrils, the growing locus for monomer addition became more ordered and hydrophobic, and could bind to HSA with stronger affinity. Besides revealing information on the binding between HSA and different Aβ42 species, the kinetics study also provided important implication concerning the potential of HSA to act as a drug for the treatment of AD. Recent studies have shown that Aβ monomer may act as a neuroprotective agent by preventing NMDA-induced exitotoxicity[65, 66]. Therefore, a drug that targets Aβ should avoid binding to Aβ monomer and preferentially binds to Aβ aggregate. Our SPR data demonstrated that the HSA-Aβ42 monomer complex was not stable and could dissociate rapidly. Therefore, when using HSA to target different Aβ species, the unwanted binding to Aβ monomer could be largely avoided. In contrast, significantly slower dissociation was observed in the case of the HSA-Aβ42 aggregate complex, suggesting that amyloid aggregates could be efficiently trapped by HSA. Therefore, the selectivity of HSA for different Aβ species suggested that HSA could be a versatile drug with the potential for treating AD patients.

HSA inhibits seeding-mediated cytotoxicity of Aβ42 aggregates

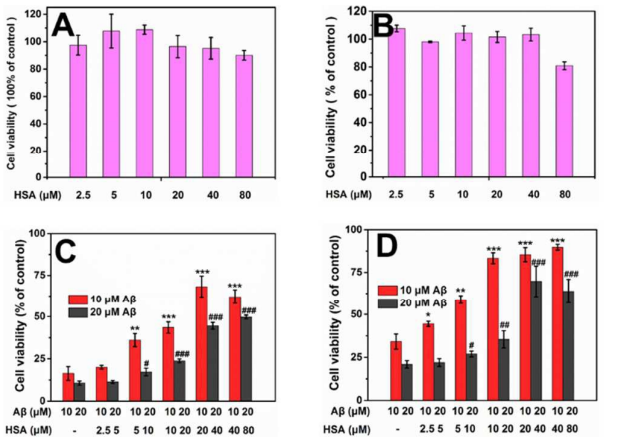

Fig. 7 HSA abolishes seeding-mediated cytotoxicity of Aβ42 in SH-SY5Y. In A (MTT assay) and B (Alamar Blue assay), HSA were added into the cells to final concentrations of 2.5, 5, 10, 20, 40 and 80 μM respectively. In C (MTT assay) and D (Alamar Blue assay), Aβ42 crude solution was added to the cells to final concentrations of 10 and 20 μM in the absence/presence of different concentrations of HSA. (one way ANOVA; *or #, $p<0.05$; **or ##, $p<0.01$; ***or ###, $p<0.001$, mean ± SD).

The neuroprotective property of HSA was investigated by examining the ability of HSA to protect SH-SY5Y against Aβ42-induced cytotoxicity using MTT reduction assay and Alamar Blue assay. First, the effect of different concentrations of HSA on SH-SY5Y cell was investigated and the results showed that HSA was not toxic to SH-SY5Y cell, and it was only at high concentration (80 μM) that obvious reduction in cellular viability was observed **(Figs. 7A & 7B)**. Recent studies have demonstrated that seeding-mediated aggregation are essential for amyloid peptide-induced cytotoxicity, including Aβ and α-synuclein[20, 24, 25, 49, 50]. Aβ42 crude (CR) solution contains predominately a mixture of Aβ42 protofibrils and monomers, and can undergo extensive fibrillation in buffer or after being added to the cells[14, 20, 49]. Moreover, Aβ42 CR can mimic the pathological situation in vivo where both Aβ monomers and protofibrils populate the brain of an AD patient as previously described[14, 49]. Therefore, treating SH-SY5Y cells with Aβ42 CR would be an appropriate way to study Aβ42 seeding-mediated cytotoxicity. Treatment of SH-SY5Y cells with 10 μM or 20 μM Aβ42 CR resulted in significant reduction in cell viability **(Figs. 7C & 7D)**. The cell viability at each concentration of Aβ42 CR was lower in the MTT assay compared to the Alamar Blue assay. The reason for this difference could be attributed to possible reduction in formation of formazan caused by Aβ in the case of the MTT assay. Despite its common use in cell viability experiments, several studies have mentioned the limitation of using MTT assay to assess cell viability induced by amyloid fibrils. A number of reasons have been put forward to explain how the reduced formation of formazan can be

induced by Aβ in the absence of overt cell death[24, 43, 67]. Alamar blue assay has been demonstrated to be an efficient method for assessing cell viability in amyloid studies[24, 48, 68]. Therefore, to obtain a more accurate effect of HSA on the cytotoxicity of Aβ, Alamar blue assay was included, and the results further confirmed that seeding-mediated Aβ aggregation was critical to the cytotoxicity induced by Aβ. Interestingly, the addition of HSA protected SH-SY5Y cells from the cytotoxicity induced by Aβ42 CR in a dose-dependent manner **(Figs. 7C & 7D)**. Moreover, HSA could inhibit the cytotoxicity of Aβ42 CR at a concentration below that of Aβ42 CR. Therefore, HSA could be considered as an efficient inhibitor for blocking seeding-mediated cytotoxicity of Aβ42. The cell viability experiments further confirmed the proposed action of HSA against Aβ42; which is, HSA targets Aβ42 aggregates to inhibit its growing process. The result also supported the suggestion that inhibitors for seeding-mediated aggregation of amyloid peptide can efficiently block its cytotoxicity[14, 25, 49].

Taken together, the results suggested that HSA could target multiple Aβ42 species on the pathway of amyloid formation to hinder their aggregation. Moreover, HSA preferentially bound to highly fibrillary and highly hydrophobic Aβ42 aggregates, forming complexes that dissociated at a slower rate than those formed between HSA and Aβ42 monomers. The ability of HSA to block the cytotoxicity of Aβ42 aggregates stemmed from its potent inhibition of the seeding process of Aβ42 aggregates **(Fig. 8)**

Despite its efficacy in blocking the aggregation and cytotoxicity of Aβ, HSA is a predominant circulating depot for many small molecules such as metal ions, fatty acid, hormones and some drugs in vivo[27, 69, 70]. Moreover, significant glycation and oxidative stress are characteristics of AD and the structure and physiological property of HSA can be impaired upon glycation and oxidation[71, 72]. Therefore, the physiological concentration of HSA in an AD brain would not be adequate to prevent the aggregation and cytotoxicity of Aβ. Peripheral depletion of Aβ monomer and shifting the equilibrium toward efflux from the brain to the plasma has been considered as a strategy for treating AD[73]. Due to its good biocompatibility, HSA is also considered as a candidate for this therapeutic strategy[42, 74]. However, as we have demonstrated in this study, HSA-Aβ monomer complex was not stable. Furthermore, Aβ monomer might have normal physiological function. Recent study has shown that the gradient of HSA across the blood-brain barrier (BBB) is not sufficient to drag Aβ out of the central nervous system (CNS)[70]. Moreover, the peripheral sink hypothesis might have some flaws and using non-antibody molecules might not reduce the Aβ in the central pool[75]. Therefore, carrying out a plasma exchange with HSA to remove the Aβ monomers and to induce the mobilization of Aβ from the CNS to the plasma might not be the best strategy to treat AD patients. It might be more logical to directly deliver HSA, which has normal physiological function, into the brain of an AD patient. Recent studies have also demonstrated that truncated HSA domain can inhibit Aβ self-association, which is more intriguing than native HSA because these subdomains of HSA might penetrate the BBB more easily[36, 76].

The pathological relevance of different Aβ species in AD remains a subject that is intensively debated and actively investigated. Despite many studies that describe Aβ fibrils as nontoxic in cell cultures, the inhibitory effect of Aβ fibrils on long-term potentiation (LTP) and the disruptive effect of amyloid fibrils formed by β2-microglobulin on the membrane of liposome have been reported [77, 78]. More importantly, recent studies have shown that the presence of Aβ fibrils is critical to the spread of Aβ deposition throughout the brains, which is an important event in the progression of AD [79-81]. In vivo studies have shown that inoculation of APP transgenic mice with the brain extract from AD patient or aged APP transgenic mice or Aβ fibrils composed of synthetic Aβ can induce the spreading of Aβ deposition [22, 23, 81]. Although the mechanism regarding the spread of Aβ deposition within the brain is not clearly established, incomplete degradation and release of Aβ fibrils from microglia have been suggested to account for the spread of Aβ deposition [82, 83]. After being transported to a new site, the Aβ fibrils fragments then act as seeds for the polymerization process and form severe amyloid deposition [83]. Therefore, inhibition of the spreading of Aβ aggregates has been suggested as a new therapeutic avenue [84]. Recent in vivo studies have suggested that seeding-mediated aggregation of Aβ is critical to the formation of Aβ fibrils and the spread of Aβ deposition in the brains and that molecules targeting seeding-mediated aggregation have therapeutic potential and may suppress the formation and spread of Aβ deposition in AD progression [14, 85]. Some small molecule drugs capable of inhibiting the seeding-mediated aggregation and cytotoxicity of Aβ have also been reported to stabilize Aβ aggregates in vivo and suppress the spread of Aβ deposition in the brains [14]. Our results showed that HSA could bind to Aβ aggregates, including Aβ fibrils and inhibit the seeding-mediated aggregation and cytotoxicity of Aβ aggregates, which suggested that HSA might have the ability to reduce the accumulation of Aβ as well as the spread of neurodegenerative pathology by binding to Aβ aggregates.

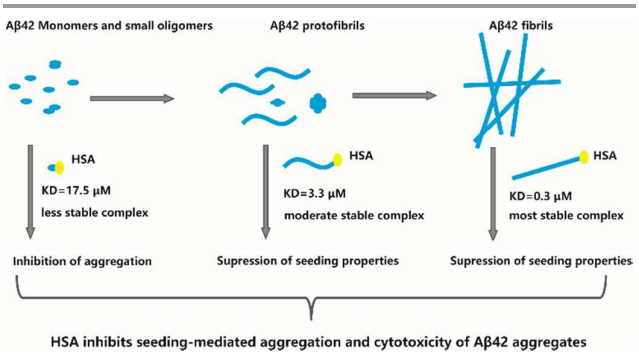

Fig. 8 Schematic representation of the possible mechanisms by which HSA inhibits the aggregation and cytotoxicity of Aβ42.

Conclusion

In summary, the current study demonstrated that HSA could target different Aβ42 species during the amyloid aggregation process, suppressing Aβ42 monomer fibrillation and seeding-mediated growth of Aβ42 protofibrils and fibrils. HSA exhibited preferential binding and increased binding affinity to Aβ42 species with increased cross β-sheet structures and hydrophobicity. Moreover, the complexes of HSA-Aβ42 amyloid were more stable, as evidenced by the much lower dissociation constant than those of HSA-Aβ42 monomer. More importantly, HSA was shown to inhibit Aβ42-induced toxicity by preventing seeding-mediated Aβ42 aggregation. This study shed new light on the underlying molecular mechanisms of HSA-modulated aggregation and toxicity of Aβ42 and this could have important implication for HSA-based therapeutic strategies for AD.

Acknowledgements

This work was supported by National Natural Science Foundation of China (No. 31100612 and 21104008) and the Fundamental Research Funds for the Central Universities (DUT10LK32 and DUT13LAB07)

Notes and references

1. C. Ballard, S. Gauthier, A. Corbett, C. Brayne, D. Aarsland and E. Jones, *Lancet*, 2011, **377**, 1019-1031.
2. D. J. Selkoe, *Physiological reviews*, 2001, **81**, 741-766.
3. C. L. Masters, G. Simms, N. A. Weinman, G. Multhaup, B. L. McDonald and K. Beyreuther, *Proceedings of the National Academy of Sciences of the United States of America*, 1985, **82**, 4245-4249.
4. D. J. Selkoe, *Science*, 2012, **337**, 1488-1492.
5. M. Shoji, T. E. Golde, J. Ghiso, T. T. Cheung, S. Estus, L. M. Shaffer, X. D. Cai, D. M. McKay, R. Tintner, B. Frangione and et al., *Science*, 1992, **258**, 126-129.
6. C. Haass, M. G. Schlossmacher, A. Y. Hung, C. Vigo-Pelfrey, A. Mellon, B. L. Ostaszewski, I. Lieberburg, E. H. Koo, D. Schenk, D. B. Teplow and et al., *Nature*, 1992, **359**, 322-325.
7. M. Goedert and M. G. Spillantini, *Science*, 2006, **314**, 777-781.
8. W. J. Strittmatter, *Science*, 2012, **335**, 1447-1448.
9. E. McGowan, F. Pickford, J. Kim, L. Onstead, J. Eriksen, C. Yu, L. Skipper, M. P. Murphy, J. Beard, P. Das, K. Jansen, M. Delucia, W. L. Lin, G. Dolios, R. Wang, C. B. Eckman, D. W. Dickson, M. Hutton, J. Hardy and T. Golde, *Neuron*, 2005, **47**, 191-199.
10. A. E. Roher, J. D. Lowenson, S. Clarke, A. S. Woods, R. J. Cotter, E. Gowing and M. J. Ball, *Proceedings of the National Academy of Sciences of the United States of America*, 1993, **90**, 10836-10840.
11. J. Hardy, *J Neurochem*, 2009, **110**, 1129-1134.
12. K. G. Mawuenyega, W. Sigurdson, V. Ovod, L. Munsell, T. Kasten, J. C. Morris, K. E. Yarasheski and R. J. Bateman, *Science*, 2010, **330**, 1774.
13. G. Meisl, X. Yang, E. Hellstrand, B. Frohm, J. B. Kirkegaard, S. I. Cohen, C. M. Dobson, S. Linse and T. P. Knowles, *Proceedings of the National Academy of Sciences of the United States of America*, 2014, **111**, 9384-9389.
14. S. Eleuteri, S. Di Giovanni, E. Rockenstein, M. Mante, A. Adame, M. Trejo, W. Wrasidlo, F. Wu, P. C. Fraering, E. Masliah and H. A. Lashuel, *Neurobiology of disease*, 2015, **74**, 144-157.
15. A. Jan, D. M. Hartley and H. A. Lashuel, *Nature protocols*, 2010, **5**, 1186-1209.
16. S. I. Cohen, S. Linse, L. M. Luheshi, E. Hellstrand, D. A. White, L. Rajah, D. E. Otzen, M. Vendruscolo, C. M. Dobson and T. P. Knowles, *Proceedings of the National Academy of Sciences of the United States of America*, 2013, **110**, 9758-9763.
17. H. A. Scheidt, I. Morgado, S. Rothemund, D. Huster and M. Fandrich, *Angewandte Chemie*, 2011, **50**, 2837-2840.
18. I. Kheterpal, M. Chen, K. D. Cook and R. Wetzel, *Journal of molecular biology*, 2006, **361**, 785-795.
19. A. Jan, O. Gokce, R. Luthi-Carter and H. A. Lashuel, *The Journal of biological chemistry*, 2008, **283**, 28176-28189.
20. A. Jan, O. Adolfsson, I. Allaman, A. L. Buccarello, P. J. Magistretti, A. Pfeifer, A. Muhs and H. A. Lashuel, *The Journal of biological chemistry*, 2011, **286**, 8585-8596.
21. L. C. Walker, M. I. Diamond, K. E. Duff and B. T. Hyman, *JAMA neurology*, 2013, **70**, 304-310.
22. M. Meyer-Luehmann, J. Coomaraswamy, T. Bolmont, S. Kaeser, C. Schaefer, E. Kilger, A. Neuenschwander, D. Abramowski, P. Frey, A. L. Jaton, J. M. Vigouret, P. Paganetti, D. M. Walsh, P. M. Mathews, J. Ghiso, M. Staufenbiel, L. C. Walker and M. Jucker, *Science*, 2006, **313**, 1781-1784.
23. Y. S. Eisele, T. Bolmont, M. Heikenwalder, F. Langer, L. H. Jacobson, Z. X. Yan, K. Roth, A. Aguzzi, M. Staufenbiel, L. C. Walker and M. Jucker, *Proceedings of the National Academy of Sciences of the United States of America*, 2009, **106**, 12926-12931.
24. M. Wogulis, S. Wright, D. Cunningham, T. Chilcote, K. Powell and R. E. Rydel, *J Neurosci*, 2005, **25**, 1071-1080.
25. A. L. Mahul-Mellier, F. Vercruysse, B. Maco, N. Ait-Bouziad, M. De Roo, D. Muller and H. A. Lashuel, *Cell Death Differ*, 2015, **22**, 2107-2122.
26. J. Nasica-Labouze, P. H. Nguyen, F. Sterpone, O. Berthoumieu, N. V. Buchete, S. Cote, A. De Simone, A. J. Doig, P. Faller, A. Garcia, A. Laio, M. S. Li, S. Melchionna, N. Mousseau, Y. Mu, A. Paravastu, S. Pasquali, D. J. Rosenman, B. Strodel, B. Tarus, J. H. Viles, T. Zhang, C. Wang and P. Derreumaux, *Chem Rev*, 2015, **115**, 3518-3563.
27. U. Kragh-Hansen, V. T. Chuang and M. Otagiri, *Biol Pharm Bull*, 2002, **25**, 695-704.
28. B. Bohrmann, L. Tjernberg, P. Kuner, S. Poli, B. Levet-Trafit, J. Naslund, G. Richards, W. Huber, H. Dobeli and C. Nordstedt, *The Journal of biological chemistry*, 1999, **274**, 15990-15995.
29. A. L. Biere, B. Ostaszewski, E. R. Stimson, B. T. Hyman, J. E. Maggio and D. J. Selkoe, *The Journal of biological chemistry*, 1996, **271**, 32916-32922.
30. J. Milojevic, A. Raditsis and G. Melacini, *Biophys J*, 2009, **97**, 2585-2594.
31. M. Rozga, M. Kloniecki, A. Jablonowska, M. Dadlez and W. Bal, *Biochem Biophys Res Commun*, 2007, **364**, 714-718.
32. Y. M. Kuo, T. A. Kokjohn, W. Kalback, D. Luehrs, D. R. Galasko, N. Chevallier, E. H. Koo, M. R. Emmerling and A. E. Roher, *Biochem Biophys Res Commun*, 2000, **268**, 750-756.
33. H. F. Stanyon and J. H. Viles, *The Journal of biological chemistry*, 2012, **287**, 28163-28168.

34. B. Xie, X. Li, X. Y. Dong and Y. Sun, *Langmuir*, 2014, **30**, 9789-9796.
35. J. Milojevic, V. Esposito, R. Das and G. Melacini, *J Am Chem Soc*, 2007, **129**, 4282-4290.
36. J. Milojevic and G. Melacini, *Biophys J*, 2011, **100**, 183-192.
37. A. A. Reyes Barcelo, F. J. Gonzalez-Velasquez and M. A. Moss, *J Biol Eng*, 2009, **3**, 5.
38. K. Hasegawa, K. Ono, M. Yamada and H. Naiki, *Biochemistry*, 2002, **41**, 13489-13498.
39. J. F. Ge, J. P. Qiao, C. C. Qi, C. W. Wang and J. N. Zhou, *Neurochem Int*, 2012, **61**, 1192-1201.
40. T. Zor and Z. Selinger, *Anal Biochem*, 1996, **236**, 302-308.
41. J. Luo, S. K. Warmlander, A. Graslund and J. P. Abrahams, *The Journal of biological chemistry*, 2014, **289**, 27766-27775.
42. M. Costa, A. M. Ortiz and J. I. Jorquera, *J Alzheimers Dis*, 2012, **29**, 159-170.
43. M. Fandrich, *Journal of molecular biology*, 2012, **421**, 427-440.
44. Y. Bin, X. Li, Y. He, S. Chen and J. Xiang, Acta Biochim Biophys Sin (Shanghai), 2013, 45, 570-577.
45. Y. Fezoui, D. M. Hartley, J. D. Harper, R. Khurana, D. M. Walsh, M. M. Condron, D. J. Selkoe, P. T. Lansbury, Jr., A. L. Fink and D. B. Teplow, Amyloid, 2000, 7, 166-178.
46. M. Arimon, V. Grimminger, F. Sanz and H. A. Lashuel, *Journal of molecular biology*, 2008, **384**, 1157-1173.
47. P. Droste, A. Frenzel, M. Steinwand, T. Pelat, P. Thullier, M. Hust, H. Lashuel and S. Dubel, *BMC Biotechnol*, 2015, **15**, 57.
48. V. Tougu, A. Karafin, K. Zovo, R. S. Chung, C. Howells, A. K. West and P. Palumaa, *J Neurochem*, 2009, **110**, 1784-1795.
49. H. Kroth, A. Ansaloni, Y. Varisco, A. Jan, N. Sreenivasachary, N. Rezaei-Ghaleh, V. Giriens, S. Lohmann, M. P. Lopez-Deber, O. Adolfsson, M. Pihlgren, P. Paganetti, W. Froestl, L. Nagel-Steger, D. Willbold, T. Schrader, M. Zweckstetter, A. Pfeifer, H. A. Lashuel and A. Muhs, *The Journal of biological chemistry*, 2012, **287**, 34786-34800.
50. S. Di Giovanni, S. Eleuteri, K. E. Paleologou, G. Yin, M. Zweckstetter, P. A. Carrupt and H. A. Lashuel, *The Journal of biological chemistry*, 2010, **285**, 14941-14954.
51. A. Thapa, E. R. Woo, E. Y. Chi, M. G. Sharoar, H. G. Jin, S. Y. Shin and I. S. Park, *Biochemistry*, 2011, **50**, 2445-2455.
52. D. E. Ehrnhoefer, J. Bieschke, A. Boeddrich, M. Herbst, L. Masino, R. Lurz, S. Engemann, A. Pastore and E. E. Wanker, *Nat Struct Mol Biol*, 2008, **15**, 558-566.
53. J. Homola, *Anal Bioanal Chem*, 2003, **377**, 528-539.
54. Q. Wang, N. Shah, J. Zhao, C. Wang, C. Zhao, L. Liu, L. Li, F. Zhou and J. Zheng, *Phys Chem Chem Phys*, 2011, **13**, 15200-15210.
55. S. J. Wood, B. Maleeff, T. Hart and R. Wetzel, *Journal of molecular biology*, 1996, **256**, 870-877.
56. D. Jiang, I. Rauda, S. Han, S. Chen and F. Zhou, *Langmuir*, 2012, **28**, 12711-12721.
57. G. S. Paranjape, S. E. Terrill, L. K. Gouwens, B. M. Ruck and M. R. Nichols, *J Neuroimmune Pharmacol*, 2013, **8**, 312-322.
58. M. R. Nichols, B. A. Colvin, E. A. Hood, G. S. Paranjape, D. C. Osborn and S. E. Terrill-Usery, *Biochemistry*, 2015, **54**, 2193-2204.
59. N. Benseny-Cases, M. Cocera and J. Cladera, *Biochem Biophys Res Commun*, 2007, **361**, 916-921.
60. M. Stefani, *FEBS J*, 2010, **277**, 4602-4613.
61. L. Gu, C. Liu, J. C. Stroud, S. Ngo, L. Jiang and Z. Guo, *The Journal of biological chemistry*, 2014, **289**, 27300-27313.
62. C. Cecchi and M. Stefani, *Biophys Chem*, 2013, **182**, 30-43.
63. R. Kodali and R. Wetzel, *Curr Opin Struct Biol*, 2007, **17**, 48-57.
64. C. Goldsbury, P. Frey, V. Olivieri, U. Aebi and S. A. Muller, *Journal of molecular biology*, 2005, **352**, 282-298.
65. M. L. Giuffrida, F. Caraci, B. Pignataro, S. Cataldo, P. De Bona, V. Bruno, G. Molinaro, G. Pappalardo, A. Messina, A. Palmigiano, D. Garozzo, F. Nicoletti, E. Rizzarelli and A. Copani, *J Neurosci*, 2009, **29**, 10582-10587.
66. M. Lindhagen-Persson, K. Brannstrom, M. Vestling, M. Steinitz and A. Olofsson, *PLoS One*, 2010, **5**, e13928.
67. K. Broersen, F. Rousseau and J. Schymkowitz, *Alzheimers Res Ther*, 2010, **2**, 12.
68. A. K. Sharma, S. T. Pavlova, J. Kim, J. Kim and L. M. Mirica, *Metallomics*, 2013, **5**, 1529-1536.
69. F. Kratz, *J Control Release*, 2008, **132**, 171-183.
70. M. Rozga and W. Bal, *Chem Res Toxicol*, 2010, **23**, 298-308.
71. J. Baraka-Vidot, G. Navarra, M. Leone, E. Bourdon, V. Militello and P. Rondeau, *Biochim Biophys Acta*, 2014, **1840**, 1712-1724.
72. E. Ramos-Fernandez, M. Tajes, E. Palomer, G. Ill-Raga, M. Bosch-Morato, B. Guivernau, I. Roman-Degano, A. Eraso-Pichot, D. Alcolea, J. Fortea, L. Nunez, A. Paez, F. Alameda, X. Fernandez-Busquets, A. Lleo, R. Elosua, M. Boada, M. A. Valverde and F. J. Munoz, *J Alzheimers Dis*, 2014, **40**, 643-657.
73. D. R. Dries, G. Yu and J. Herz, *Proceedings of the National Academy of Sciences of the United States of America*, 2012, **109**, 3199-3200.
74. J. Milojevic, M. Costa, A. M. Ortiz, J. I. Jorquera and G. Melacini, *J Alzheimers Dis*, 2014, **38**, 753-765.
75. S. J. Henderson, C. Andersson, R. Narwal, J. Janson, T. J. Goldschmidt, P. Appelkvist, A. Bogstedt, A. C. Steffen, U. Haupts, J. Tebbe, P. O. Freskgard, L. Jermutus, M. Burrell, S. B. Fowler and C. I. Webster, *Brain*, 2014, **137**, 553-564.
76. M. Algamal, J. Milojevic, N. Jafari, W. Zhang and G. Melacini, *Biophys J*, 2013, **105**, 1700-1709.
77. A. J. Nicoll, S. Panico, D. B. Freir, D. Wright, C. Terry, E. Risse, C. E. Herron, T. O'Malley, J. D. Wadsworth, M. A. Farrow, D. M. Walsh, H. R. Saibil and J. Collinge, Nat Commun, 2013, 4, 2416.
78. L. Milanesi, T. Sheynis, W. F. Xue, E. V. Orlova, A. L. Hellewell, R. Jelinek, E. W. Hewitt, S. E. Radford and H. R. Saibil, Proceedings of the National Academy of Sciences of the United States of America, 2012, 109, 20455-20460.
79. K. W. Tipping, P. van Oosten-Hawle, E. W. Hewitt and S. E. Radford, Trends Biochem Sci, 2015, 40, 719-727.
80. Z. Jaunmuktane, S. Mead, M. Ellis, J. D. Wadsworth, A. J. Nicoll, J. Kenny, F. Launchbury, J. Linehan, A. Richard-Loendt, A. S. Walker, P. Rudge, J. Collinge and S. Brandner, Nature, 2015, 525, 247-250.
81. J. Stohr, J. C. Watts, Z. L. Mensinger, A. Oehler, S. K. Grillo, S. J. DeArmond, S. B. Prusiner and K. Giles, Proceedings of the National Academy of Sciences of the United States of America, 2012, 109, 11025-11030.
82. A. Majumdar, H. Chung, G. Dolios, R. Wang, N. Asamoah, P. Lobel and F. R. Maxfield, Neurobiol Aging, 2008, 29, 707-715.
83. J. X. Lu, W. Qiang, W. M. Yau, C. D. Schwieters, S. C. Meredith and R. Tycko, Cell, 2013, 154, 1257-1268.
84. S. J. Lee, H. S. Lim, E. Masliah and H. J. Lee, Neurosci Res, 2011, 70, 339-348.

85. B. Frost and M. I. Diamond, Nat Rev Neurosci, 2010, 11, 155-159.

Graphic abstract

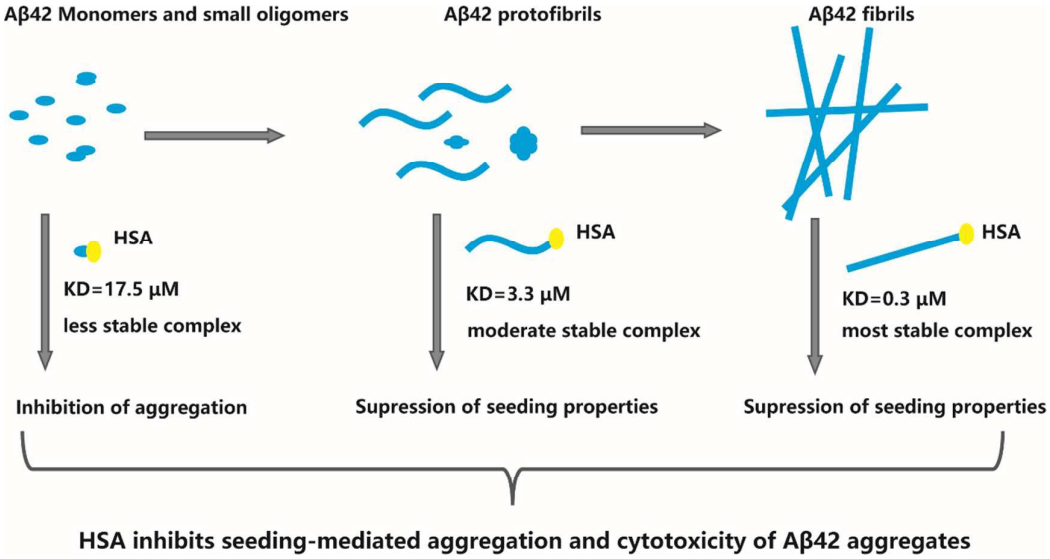

HSA inhibits Aβ42 fibrillation and cytotoxicity through interfering with different stages of Aβ42 fibrillation and targeting different Aβ42 intermediate aggregates.